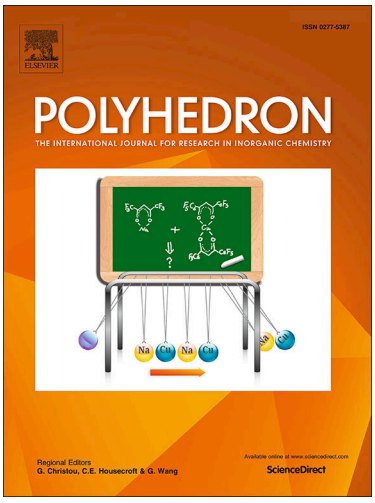


# Copper(II) Complexes Containing *N′* -Aromatic Group Substituted *N*,*N′* ,*N*-bis((3,5-dimethyl-1H-pyrazol-1-yl)methyl)amines: Synthesis, Structures, Polymerization of Methyl Methacrylate and Ring Opening Polymerization of *rac*-Lactide

Hyungwoo Cho, Solhye Choe, Dongil Kim, Hyosun Lee, Saira Nayab

PII: S0277-5387(20)30298-9
DOI: https://doi.org/10.1016/j.poly.2020.114641
Reference: POLY 114641

To appear in: *Polyhedron*

Received Date: 18 April 2020
Revised Date: 29 May 2020
Accepted Date: 31 May 2020

Please cite this article as: H. Cho, S. Choe, D. Kim, H. Lee, S. Nayab, Copper(II) Complexes Containing *N′* -Aromatic Group Substituted *N*,*N′* ,*N*-bis((3,5-dimethyl-1H-pyrazol-1-yl)methyl)amines: Synthesis, Structures, Polymerization of Methyl Methacrylate and Ring Opening Polymerization of *rac*-Lactide, *Polyhedron* (2020), doi: https://doi.org/10.1016/j.poly.2020.114641

***Revised***

# Copper(II) Complexes Containing *N′*-Aromatic Group Substituted *N*,*N′*,*N*-bis((3,5-dimethyl-1H-pyrazol-1-yl)methyl)amines: Synthesis, Structures, Polymerization of Methyl Methacrylate and Ring Opening Polymerization of *rac*-Lactide

**Hyungwoo Cho,[a] Solhye Choe,[a] Dongil Kim,[a] Hyosun Lee,[a,*] and Saira Nayab[b,*]**

[a]*Department of Chemistry and Green-Nano Materials Research Center, Kyungpook National University, 80 Daehakro, Bukgu, Daegu, 41566, Republic of Korea*

**E-mail address: hyosunlee@knu.ac.kr*

[b]*Department of Chemistry, Shaheed Benazir Bhutto University, Sheringal Dir (U), Khyber Pakhtunkhwa, Islamic Republic of Pakistan*

**E-mail address: drnayab@sbbu.edu.pk, sairanayab07@yahoo.com*

---

*Corresponding authors. Tel: +82-53-950-5337; fax: +82-53-950-6330

E-mail address: *hyosunlee@knu.ac.kr*

Email address: *drnayab@sbbu.edu.pk, sairanayab07@yahoo.com*

# Copper(II) Complexes Containing *N*′-Aromatic Group Substituted *N*,*N*′,*N*-Bis((3,5-dimethyl-1*H*-pyrazol-1-yl)methyl)amines: Synthesis, Structures, Polymerization of Methyl Methacrylate, and Ring-Opening Polymerization of *rac*-Lactide


## Abstract

A series of Cu(II) complexes, **[$L_nCuCl_2$]** ($L_n$ = $L_A$–$L_F$), supported by *N*′-aromatic-group-substituted *N*,*N*-bis((3,5-dimethyl-1*H*-pyrazol-1-yl)methylamine ligands have been synthesized. Variations of substituents at the *ortho* position of the aniline moiety influenced the solid-state structures of these complexes. The X-ray structures of **[$L_nCuCl_2$]** ($L_n$ = $L_A$–$L_C$ and $L_F$) revealed that ligands are coordinated in a *N*,*N*,*N*-tridentate fashion to Cu(II) center and adopted a distorted square-pyramidal geometry, while **[$L_DCuCl_2$]** with *N*,*N*-bidentate coordination adopts distorted tetrahedral geometry. These complexes were capable of polymerizing methyl methacrylate (MMA) in the presence of modified methylaluminoxane (MMAO), with **[$L_FCuCl_2$]** displaying the highest activity ($2.81 \times 10^4$ g PMMA (mol Cu)$^{-1}$ h$^{-1}$). Regardless of ligand architecture, syndio-enriched PMMAs have been furnished with a slightly broader polydispersity index (PDI). Additionally, the *in situ* generated dimethyl derivatives, polymerized *rac*-LA and furnished PLA with mediocre heterotacticities at room temperature. Importantly, the catalytic efficiencies of the Cu(II) complexes studied have been found to be influenced by the steric and electronic properties of ligand.


***Keywords:*** Pyrazolyl-methylamines; Copper complexes; Square-pyramidal geometry; Tetrahedral geometry; Syndiotactic PMMA; Heterotactic PLA

## 1. Introduction

Pyrazole-based ligands have attracted a great deal of attention as a powerful chelating tool in a wide array of transition-metal complexes [1-4]. The success of pyrazolyl-based ligands arise from their easy synthetic approach and various modifications of their linker units composed of two or three pyrazole moieties [5-7], which enables the construction of diverse coordination geometries and significant nuclearities [8,9]. Since the pioneering work of Driessen in 1982 [10], a variety of *N*-substituted bis-pyrazolyl ligands and their transition-metal complexes have been investigated successfully in numerous catalytic transformations. For instance, they have been studied as supramolecules for metal–organic frameworks (MOF) [6], catalysts for organic transformations [11,7], and as bioinorganic materials in pharmaceutical preparations [12,13]. They have also been utilized as metal-ion extractants [14], antibacterial agents [15,16], cancer sensors and oxidation agents [17].

More recently, *N*-substituted pyrazolyl amines ligated to a variety of late transition metals such as Pt(II), Pd(II), Ru(II), Rh(I), Ni(II), Zn(II), and Co(II) have demonstrated useful catalytic properties in olefins [18-20] and in methyl methacrylate (MMA) polymerizations [21-23]. Early transition-metal complexes generally cannot tolerate polar functional groups due to the highly electron-deficient nature of the metal center. Late-transition-metal complexes overcome this drawback and demonstrate better polymerization of polar monomers in a controlled fashion, owing to their less-oxophilic nature [24-28]. Recently, our group has been involved in the synthesis of late transition metal based initiators supported by the *N*,*N*-bis(1*H*-pyrazolyl-1-methyl)aniline ligand and its derivatives for MMA and *rac*-LA polymerizations. These catalyst showed promising activities and furnished polymers, PMMAs and PLAs, with moderate to high stereoselectivities [29-34]. Yu et al. [35], Kang et al. [36] and Lian group [4] have reported similar results showing that pyrazolyl zinc complexes are active initiators for the ring-opening polymerization (ROP) of LA because the pyrazole

motif offers highly electrophilic metal centers. However, thus far, Cu(II) complexes supported by bis-pyrazolyl amine-based ligands have been less extensively investigated for MMA and *rac*-LA polymerizations. Consequently, given the importance of bis-pyrazolyl-methylamine ligands and taking into consideration the promising results obtained by our group [29-34], we herein studied the synthesis of Cu(II) complexes based on *N*′-aromatic-group-substituted *N*,*N*′,*N*-bis((3,5-dimethyl-1*H*-pyrazol-1-yl)methyl)amine ligands, and explored their catalytic efficacies toward MMA and *rac*-LA polymerizations.

## 2. Experimental

### *2.1. Materials*

The synthesis of all ligands and their corresponding Cu(II) complexes were carried out using bench top techniques. The polymerization reactions were carried out using a high-vacuum Schlenk line and glovebox. Copper(II) chloride dihydrate ($CuCl_2 \cdot 2H_2O$), 3,5-dimethylpyrazole, *para*-formaldehyde, aniline, 4-methoxyaniline, 4-fluoroaniline, 2,4,6-trimethylaniline, 2,6-diethylaniline, 4-isopropylaniline, magnesium sulfate ($MgSO_4$), and molecular sieves (0.4 nm) were purchased from Sigma-Aldrich. Anhydrous solvents such as ethanol (EtOH), acetonitrile ($CH_3CN$), *n*-hexane (*n*-Hex), diethyl ether ($Et_2O$), and dimethylformamide (DMF) were purchased from Sigma-Aldrich and were used without further purification. THF and toluene were dried over benzophenone ketyl radical, whereas $CH_2Cl_2$ was dried over calcium hydride ($CaH_2$); all of these solvents were deoxygenated by distillation under argon before use. MMA dried over molecular sieves and was distilled under reduced pressure before use. Modified methylaluminoxane (MMAO) was purchased from Tosoh Finechem Corporation as 5.90 wt% aluminum in toluene solution and was used without further purification. 3,5-Dimethyl-1*H*-pyrazolyl-1-methanol was prepared as reported previously [37]. $\mathbf{L_A}$ (*N*,*N*-Bis((3,5-

dimethyl-1*H*-pyrazol-1-yl)methyl)aniline) [29,30,38], $\mathbf{L_B}$ (*N*,*N*-Bis((3,5-dimethyl-1*H*-pyrazol-1-yl)methyl)-4-methoxyaniline) [31,39], $\mathbf{L_C}$ *N*,*N*-Bis((3,5-dimethyl-1*H*-pyrazol-1-yl)methyl)-4-fluoroaniline [31,39], $\mathbf{L_D}$ (*N*,*N*-Bis((3,5-dimethyl-1*H*-pyrazol-1-yl)methyl)-2,4,6-trimethylaniline) [31] and $\mathbf{L_E}$ (*N*,*N*-Bis((3,5-dimethyl-1*H*-pyrazol-1-yl)methyl)-2,6-diethylaniline) [30] were synthesized according to the previously reported protocols.

*2.2. Instrumentation*

Elemental analysis (C, H, N) of the synthesized Cu(II) complexes was carried out using an elemental analyzer (EA 1108; Carlo-Erba, Milan, Italy). The $^{1}$H NMR (500 MHz) and $^{13}$C NMR (125 MHz) spectra were recorded on a Bruker Avance digital NMR spectrometer. Chemical shifts are reported in ppm relative to the signal of tetramethylsilane ($SiMe_4$) as an internal standard; coupling constants are reported in Hertz (Hz). Data are recorded as m = multiplet, br = broad, s = singlet, d = doublet, t = triplet, and q = quartet. Fourier transform Infrared (FTIR) spectra were recorded on a Bruker FT/IR-Alpha spectrometer (neat), and the data are reported in wavenumbers ($cm^{1}$). The number average molecular weights ($M_n$) and polydispersity index (PDI) values of the obtained poly(methyl methacrylate) (PMMA) were measured using gel-permeation chromatography (GPC) (THF, Alliance 1200S, Waters Corp., Milford, MA). The glass-transition temperature ($T_g$) of PMMA was measured using a thermal analyzer (DSC 4000; Perkin-Elmer). The microstructural analysis of PMMA as syndiotactic (*rr*, 0.85 ppm), heterotactic (*mr*, 1.02 ppm), or isotactic (*mm*, 1.21 ppm) was carried out by $^{1}$H NMR (**Figure S4**) [40,41]. GPC analysis of PLA samples was performed at 25 °C on a Waters Alliance GPCV2000 equipped with differential refractive index detectors and calibrated using monodisperse polystyrene (PS) standards; THF was used as the eluent at a flow rate of 1.0 mL/min. $M_n$ and PDI values of polymers are given relative to those of PS standards. The

stereochemistry of the PLA formed was determined by homodecoupled $^1$H NMR spectra of the polymers (**Figure S16**) [42,43].

*2.3. Synthetic procedures*

*2.3.1. N,N-Bis((3,5-dimethyl-1H-pyrazol-1-yl)methyl)-4-isopropylaniline ($L_F$)*

The $CH_2Cl_2$ solution (50.0 mL) of 4-isopropylaniline (3.00 mL, 20.0 mmol) was added to a $CH_2Cl_2$ solution (50.0 mL) of 3,5-dimethylpyrazole-1-methanol (5.05 g, 40.0 mmol), and the resultant mixture was stirred at room temperature for 24 h. The mixture was dried over $MgSO_4$ and concentrated under reduced pressure. The crude liquid was subjected to vacuum distillation to give a yellow oil as the final liquid (6.06 g, 76%). $^1$H NMR ($CDCl_3$, 500 MHz): $\delta$ 7.09 (d, 2H, $J$ = 8.39 Hz, –$C_6$**H**$_4$–), 6.95 (d, 2H, $J$ = 8.70 Hz, –$C_6$**H**$_4$–), 5.73 (s, 2H, –N–C**(**$CH_{3)}$)=C**H**–C**(**$CH_3$)=N–), 5.46 (s, 4H, –N–C**H**$_2$–N–), 2.85–2.80 (m, 1H, iso-$C_3$**H**$_7$–), 2.20 (s, 6H, –N–C**(**C**H**$_{3)}$)=CH–C**(**$CH_3$)=N–), 2.01 (s, 6H, –N–C($CH_{3)}$)=CH–C**(**C**H**$_3$)=N–), 1.20 (d, 6H, $J$ = 6.87, Hz iso-$C_3$**H**$_7$). $^{13}$C NMR ($CDCl_3$, 125 MHz): $\delta$ 147.15 (s, 2C, –N–C**(**$CH_{3)}$)=CH–**C(**$CH_3$)=N–), 143.93 (s, 1C, –**C**$_6$H$_4$–), 143.07 (s, 1C, –**C**$_6$H$_4$–), 139.0 (s, 2C, –N–C**(**$CH_{3)}$)=CH–**C(**$CH_3$)=N–), 126.5 (d, 2C, $J$ = 156.2 Hz, –**C**$_6$H$_4$–), 120.9 (d, 2C, $J$ = 164.39 Hz, –**C**$_6$H$_4$–) 105.2 (d, 2C, $J$ =172.6 Hz, –N–C**(**$CH_{3)}$)=**C**H–C**(**$CH_3$)=N–), 64.2 (t, 2C, $J$ = 300.6 Hz, –N–**C**$H_2$–N–), 32.9 (d, 1C, $J$ = 138.9 Hz, iso-**C**$_3$H$_7$), 23.6 (q, 2C , $J$ = 376.9 Hz, iso-**C**$_3$H$_7$), 13.2 (q, 2C, $J$ = 344.2 Hz, –N–C**(**$CH_{3)}$)=CH–C**(**C**H**$_3$)=N–), 10.4 (q, 2C, $J$ = 348.7 Hz, –N–C**(**C**H**$_{3)}$)=CH–C**(**$CH_3$)=N–). Analysis calculated for $C_{21}H_{29}N_5$ (%): C, 71.7, H, 8.32, N, 19.9. Found: C, 72.2, H, 8.43, N, 19.8. IR (oily liquid neat; $cm^{-1}$): ν(C–H) 2961 w; ν(C = C) 1547 s; ν(C = C) + ν (C = N) /pz ring, 1519 s, 1454 s; $\nu_{bend}$(–C–H $sp^3$) 1403 m; ν(N–C) 1225 s; $\nu_{bend}$(C–H $sp^2$) 809 w.

*2.3.2 N,N-Bis((3,5-dimethyl-1H-pyrazol-1-yl)methyl)aniline copper(II) chloride ([$L_A$CuCl$_2$])*

A solution of $\mathbf{L_A}$ (0.619 g, 2.00 mmol) in dried EtOH (20.0 mL) was treated with an EtOH solution of $CuCl_2 \cdot 2H_2O$ (0.341 g, 2.00 mmol), and the resulting mixture was stirred at room temperature for 12 h. The blue-green precipitate was filtered, washed with cold EtOH (50.0 mL × 2), followed by subsequent washing with cold $Et_2O$ (50.0 mL × 2) to obtain **[$\mathbf{L_A}$CuCl$_2$]** as the final product (0.719 g, 81%). The X-ray-quality single crystals were obtained by layering *n*-hexane over a $CH_2Cl_2$ solution of **[$\mathbf{L_A}$CuCl$_2$]**. Analysis calculated for $C_{19}H_{25}Cl_2N_5CuO$ (%): C, 48.7, H, 5.22, N, 15.8. Found: C, 48.7, H, 5.29, N, 15.8. IR (solid neat; $cm^{-1}$): ν(C–H) 2921 w; ν(C=C) 1598 s; ν(C=C) + ν(C=N) /pz ring, 1549 s, 1506 s; $\nu_{bend}$(–C–H $sp^3$) 1454 m; ν(N–C) 1211 s; $\nu_{bend}$(C–H $sp^2$) 816 w.

*2.3.3 N,N-Bis((3,5-dimethyl-1H-pyrazol-1-yl)methyl)-4-methoxyaniline copper(II) chloride ([$L_B$CuCl$_2$])*

A method analogous to that described for the preparation of **[$\mathbf{L_A}$CuCl$_2$]** was used to prepare **[$\mathbf{L_B}$CuCl$_2$]**; in this case, $\mathbf{L_B}$ (0.677 g, 2.00 mmol) and $CuCl_2 \cdot 2H_2O$ (0.341 g, 2.00 mmol) were used to obtain a blue solid (0.740 g, 78%). The X-ray-quality single crystals were obtained by layering *n*-hexane over a $CH_2Cl_2$ solution of **[$\mathbf{L_B}$CuCl$_2$]**. Analysis calculated for $C_{19}H_{25}Cl_2N_5CuO$ (%): C, 48.1, H, 5.32, N, 14.8. Found: C, 47.2, H, 5.28, N, 14.7. IR (solid neat; $cm^{-1}$): ν(C–H) 2956 w; ν(C=C) 1554 s; ν(C=C) + ν(C=N) /pz ring, 1510 s, 1465 s; $\nu_{bend}$(–C–H $sp^3$) 1465 m; ν(N-C) 1249 s; $\nu_{bend}$(C-H $sp^2$) 810 w.

**2.3.4 *N,N-Bis((3,5-dimethyl-1H-pyrazol-1-yl)methyl)-4-fluoroaniline copper(II) chloride ([$L_C$CuCl$_2$])***

A method analogous to that used to prepare **[$\mathbf{L_A}$CuCl$_2$]** was adopted for the synthesis of **[$\mathbf{L_C}$CuCl$_2$]**; in this case, $\mathbf{L_C}$ (0.507 g, 2.00 mmol) and $CuCl_2 \cdot 2H_2O$ (0.341 g, 2.00 mmol) were used

to obtain a dark-green solid (0.636 g, 82%). The green crystals suitable for X-ray analysis were obtained by layering *n*-hexane over a $CH_2Cl_2$ solution of **[$L_C$CuCl$_2$]**. Analysis calculated for $C_{18}H_{22}Cl_2N_5CuF$ (%): C, 46.8, H, 4.80, N, 15.2. Found: C, 46.4, H, 4.86, N, 15.3. IR (solid neat; $cm^{-1}$): ν(C–H) 3051 w; ν(C=C) 1553 s; ν(C=C) + ν(C=N) /pz ring, 1510 s, 1465 s; $\nu_{bend}$(–C–H $sp^3$) 1399 m; ν(N–C) 1214 s; $\nu_{bend}$(C–H $sp^2$) 859 w.

*2.3.5 N,N-Bis((3,5-dimethyl-1H-pyrazol-1-yl)methyl)-2,4,6-trimethylaniline copper(II) chloride ([$L_D$CuCl$_2$])*

A method analogous to that described for **[$L_A$CuCl$_2$]** was used to synthesize **[$L_D$CuCl$_2$]**; in this case, utilizing **$L_D$** (0.703 g, 2.00 mmol) and $CuCl_2 \cdot 2H_2O$ (0.341 g, 2.00 mmol) to get pale green solid (0.729 g, 75%). The green cubic X-ray-quality single crystals were obtained by layering *n*-hexane over a $CH_2Cl_2$ solution of **[$L_D$CuCl$_2$]**. Analysis calculated for $C_{22}H_{31}Cl_4N_5Cu$ (%): C, 46.3, H, 5.47, N, 12.3. Found: C, 46.2, H, 5.46, N, 12.6. IR (solid neat; $cm^{-1}$): ν(C-H) 2913 w; ν(C = C) 1552 s; ν(C = C) + ν (C = N) /pz ring, 1486 s, 1459 s; $\nu_{bend}$(-C-H $sp^3$) 1418 m; ν(N-C) 1221 s; $\nu_{bend}$(C-H $sp^2$) 827 w.

*2.3.6 N,N-Bis((3,5-dimethyl-1H-pyrazol-1-yl)methyl)-2,6-diethylaniline copper(II) chloride ([$L_E$CuCl$_2$])*

A method analogous to that described for **[$L_A$CuCl$_2$]** was adopted for the synthesis of **[$L_E$CuCl$_2$]**; in this case, **$L_E$** (0.731 g, 2.00 mmol) and $CuCl_2 \cdot 2H_2O$ (0.341 g, 2.00 mmol) were used to obtain a green solid as the final product (0.700 g, 70%). Analysis calculated for $C_{21}H_{29}Cl_2N_5Cu$ (%): C, 52.9, H, 6.25, N, 14.0. Found: C, 53.0, H, 6.37, N, 14.6. IR (solid neat; $cm^{-1}$): ν(C–H) 3195 w; ν(C=C) 1568 s; ν(C=C) + ν(C=N) /pz ring, 1512 s, 1470 s; $\nu_{bend}$(–C–H $sp^3$) 1411 m; ν(N-C) 1278 s; $\nu_{bend}$(C-H $sp^2$) 818 w.

*2.3.7 N,N-Bis((3,5-dimethyl-1H-pyrazol-1-yl)methyl)-4-isopropylaniline copper(II) chloride ([$L_F CuCl_2$])*

A method analogous to that described for **[$L_A CuCl_2$]** was adopted for the synthesis of **[$L_F CuCl_2$]**; in this case, **$L_F$** (0.507 g, 2.00 mmol) and $CuCl_2 \cdot 2H_2O$ (0.341 g, 2.00 mmol) were used to obtain a green solid as the final product (0.636 g, 82%). The X-ray-quality single crystals were obtained by layering *n*-hexane over a $CH_2Cl_2$ solution of **[$L_F CuCl_2$]**. Analysis calculated for $C_{21}H_{29}Cl_2N_5Cu$ (%): C, 51.9, H, 6.02, N, 14.4. Found: C, 51.4, H, 6.22, N, 13.8. IR (solid neat; $cm^{-1}$): ν(C–H) 2959 w; ν(C=C) 1552 s; ν(C=C) + ν(C=N) /pz ring, 1509 s, 1462 s; $\nu_{bend}$(–C–H $sp^3$) 1391 m; ν(N–C) 1210 s; $\nu_{bend}$(C–H $sp^2$) 808 w.

## 2.4. MMA polymerization

In a Schlenk flask (100 mL), **[$L_A CuCl_2$]** (6.66 mg, 15.0 μmol), **[$L_B CuCl_2$]** (7.11 mg, 15.0 μmol), **[$L_C CuCl_2$]** (6.93 mg, 15.0 μmol), **[$L_D CuCl_2$]** (7.29 mg, 15.0 μmol), **[$L_E CuCl_2$]** (7.50 mg, 15.0 μmol), or **[$L_F CuCl_2$]** (7.29 mg, 15.0 μmol) was dissolved in toluene (10.0 mL). MMAO (5.90 wt% in toluene, 3.80 mL, $[MMAO]_0/[Cu(II)\ catalyst]_0$ = 500) under a dry argon atmosphere was transferred to the aforementioned mentioned solution. After the mixture had been stirred at 60 °C for 20 min, it was transferred into an MMA (5.00 mL, 47.1 mmol, $[MMA]_0/[M(II)\ catalyst]_0$ = 3100) solution. The reaction flask was immersed in an oil bath at 60 °C, and the mixture was stirred for 2 h. The resulting polymer was precipitated in MeOH (500 mL) and HCl (5.00 mL) with stirring for 1 h. The polymer was filtered and subsequently washed with MeOH (100 mL × 3) to give PMMA, which was dried under vacuum at 60 °C.

## 2.5. *rac*-Lactide polymerization

In a general polymerization reaction for *rac*-LA with the dimethyl copper initiators, the active catalytic species were generated as follows. Dichloro Cu(II) complexes, i.e., **[$L_A$CuCl$_2$]** (0.222 g, 0.50 mmol), **[$L_B$CuCl$_2$]** (0.237 g, 0.50 mmol), **[$L_C$CuCl$_2$]** (0.231 g, 0.50 mmol), **[$L_D$CuCl$_2$]** (0.243 g, 0.50 mmol), **[$L_E$CuCl$_2$]** (0.250 g, 0.50 mmol), or **[$L_F$CuCl$_2$]** (0.243 g, 0.50 mmol), and dried THF (7.35 mL) were added to a 100 mL Schlenk flask under an argon atmosphere. To this solution was added MeLi (1.00 mmol, 0.65 mL of a 1.6 *M* solution in $Et_2O$) dropwise to generate *in situ* dimethyl Cu(II) species. After the mixture was stirred for 2 h at room temperature, the resulting THF solution of a dimethyl Cu(II) complex, i.e. **[$L_n$CuMe$_2$]** ($L_n$ = $L_A$–$L_F$), was used as an initiator for the ROP of *rac*-LA.

The general procedure for the polymerization reaction was as follows. A Schlenk flask (100 mL) was charged with *rac*-LA (0.901 g, 6.25 mmol) under argon atmosphere, and 5.00 mL of dried $CH_2Cl_2$ was added to completely solubilize the monomer. The polymerization was initiated by slow addition of the catalyst solution (1.0 mL, 0.0625 mmol) *via* a syringe under argon at 25 °C into monomer solution. The reaction mixture was stirred for the specified time and the polymerization reactions were quenched by using $H_2O$ (1.0 mL) followed by the addition of *n*-hexane (2.0 mL) and the solvent was evaporated directly to give sticky polymeric material. The resultant polymeric residue was subjected to monomer conversion determination, which was monitored by integrating monomer versus polymer methine resonances in $^1$H NMR spectrum; $^1$H NMR ($CDCl_3$, 500 MHz) for the obtained polymer: $\delta$ 5.13-5.20 (m, 1H), 1.50-1.62 (m, 3H). The precipitates collected from the bulk mixture were again dissolved with $CH_2Cl_2$, and sequentially precipitated into n-hexane. Solvents were decanted and the white solids were dried *in vacuo* at 40 °C for 12 h.

### 2.6. X-ray crystallographic studies

X-ray-quality single crystals of **[$L_nCuCl_2$]** ($L_n$ = $L_A$–$L_D$ and $L_F$) were coated with Paratone-N oil, and the diffraction data were collected at 100(2) K using synchrotron radiation ($\lambda$ = 0.700 Å) on an ADSC Quantum-210 detector at 2D SMC with a silicon (111) double-crystal monochromator (DCM) at the Pohang Accelerator Laboratory, South Korea. The PAL BL2D-SMDC program [44] was used for data collection (the detector distance was 63 mm, omega scan; $\Delta\omega$ = 1°, exposure time was 1 sec per frame); HKL3000sm (Ver. 703r) [45] was used for cell refinement, reduction, and absorption correction. A green cubic-shaped crystal of the complexes were picked up with Paratone-N oil and mounted onto a Bruker SMART CCD diffractometer equipped with a graphite-monochromated Mo-Kα ($\lambda$ = 0.71073 Å) radiation source; data were collected with the samples under a $N_2$ cold stream (200(2) K) at the Western Seoul Center of Korea Basic Science Institute. Data collection and integration were performed with the SMART (Bruker, 2000) and SAINT-Plus (Bruker, 2001) software packages [46]. Semi-empirical absorption corrections based on equivalent reflections were applied by SADABS [47]. All measured structures were solved by dual-space algorism related with intrinsic phasing using the SHELXT-2018/2 [48] program and were refined by full-matrix least-squares refinement using the SHELXL-2018/3 [49] program. The positions of all non-hydrogen atoms were refined with anisotropic displacement factors. All hydrogen atoms were placed using a riding model, and their positions were constrained relative to the positions of their parent atoms using the appropriate HFIX command in the SHELXL-2018/3 program. The crystallographic refinements and structural data are summarized in **Table S1**.

## 3. Results and Discussion

### *3.1. Synthesis and physical parameters*

The ligands were obtained *via* a single-step condensation reaction of the aniline derivatives and 3,5-dimethyl-1*H*-pyrazolyl-1-methanol in $CH_2Cl_2$ (**Scheme 1**). In the $^1$H NMR spectrum of $\mathbf{L_F}$,

the protons of the $–CH_2–$ linker units of 3,5-dimethylpyrazole and aniline were observed at $\delta$ 5.46 ppm (**Figure S1**). The *meta* and *ortho* protons of 4-isopropylaniline appeared at $\delta$ 7.09 and 6.95 ppm, respectively. The –CH– protons of the isopropyl group and $–CH_3$ groups appeared at $\delta$ 2.80 and 2.20 ppm, respectively. Similarly, the $^{13}C$ NMR spectrum (**Figure S2**) of $\mathbf{L_F}$ shows representative peaks consistent with the ligand formulation. The Cu(II) complexes were synthesized *via* coordination of ligands ($L_n = L_A–L_F$) with $CuCl_2 \cdot 2H_2O$ in a 1:1 molar ratio in anhydrous EtOH in facile yields and purity (**Scheme 1**).

Spectroscopic characterization by FTIR confirmed the synthesis of the Cu(II) complexes. The characteristic peaks observed in the FTIR spectra of $\mathbf{[L_nCuCl_2]}$ ($L_n = L_A–L_F$) lie in the expected range. For instance, the common absorption bands for $\nu$(C=C) + $\nu$(C=N) of the pyrazole rings appread at ~1512 and ~1479 $cm^{-1}$, whereas the aromatic C–H and C=C stretching bands appeared at ~3207–2961 and ~1579–1552 $cm^{-1}$, respectively [50]. In addition, typical $sp^3$ and $sp^2$ C–H bending bands appeared at frequencies consistent with those reported in the literature. The FTIR spectra of the complexes showed that the peaks corresponding to aromatic C=C stretching and aromatic C–H bands shifted from lower wavenumbers to higher wavenumbers compared with the peaks of their corresponding ligands. The effect of ring substituents on νN-C and $\nu_{sym}CH_3$ is observed to be small. However, the $\nu_{sym}CH_3$ stretching frequencies increases as ring substituents become more electron donating particularly at *ortho* position, as evident from the perturbed νN-C (1221 to 1278 $cm^{-1}$) and $\nu_{sym}CH_3$ frequencies. The bulkier alkyl group results in vibrations occurred at slightly higher frequencies (3138-3219 $cm^{-1}$ for 2,6-diethyl substituent in $\mathbf{[L_ECuCl_2]}$) compared to less bulkier groups (2718-2913 $cm^{-1}$, for 2,6-dimethyl substituents in $\mathbf{[L_DCuCl_2]}$). Additionally, the presence of 2,6-dimethyl substituents on the aniline ring perturbed the binding of the ligand to metal centre and resulted in bidentate instead of tridentate. At same time the anticipated increase in the perturbed νN-C

(1278 $cm^{-1}$) and $\nu_{sym}CH_3$ (3138-3219 $cm^{-1}$) for 2,6-diethyl substituents at aniline moiety in **[$L_E$CuCl$_2$]** might reflect the bidentate coordination mode.

The elemental analysis results for the synthesized complexes are consistent with the formula proposed in **Scheme 1** and confirm the purity of the isolated complexes. All of the synthesized Cu(II) complexes **[$L_n$CuCl$_2$]** ($L_n$ = $L_A$–$L_F$) were found to be stable and can be stored at room temperature for months without appreciable degradation.

*3.2. Molecular structures of Cu(II) complexes*

Single-crystal X-ray diffraction studies were performed to determine the geometries of Cu(II) complexes. The ORTEP diagrams of **[$L_n$CuCl$_2$]** ($L_n$ = $L_A$–$L_D$ and $L_F$) are shown in **Figs. 1–5**, and selected bond lengths and angles are listed in **Table 1**. Complexes, **[$L_A$CuCl$_2$]**, **[$L_B$CuCl$_2$]**, **[$L_C$CuCl$_2$]**, **[$L_D$CuCl$_2$]**, and **[$L_F$CuCl$_2$]** crystallized in monoclinic systems with $P2_12_12_1$, $P2_1/c$, $C2/c$, $P$-1, and $P2_1/n$ space groups, respectively.

Cu(II) complexes **[$L_n$CuCl$_2$]** ($L_n$ = $L_A$–$L_C$ and $L_F$) exhibited distorted square-pyramidal geometries around a Cu(II) center *via* tridentate coordination to an *N*-substituted bis-pyrazolyl ligand, along with monodentate coordination to two chloro ligands. The M–$N_{pyrazole}$ and Cu–Cl lengths in **[$L_n$CuCl$_2$]** ($L_n$ = $L_A$–$L_C$ and $L_F$) lie in 2.257(9)–2.383(9) Å and 1.981(4)–2.011(3) Å ranges and are not strongly affected by the *para* substituents of the aniline moieties. These structural parameters agreed well with the expected values based on the parameters of similar complexes [3]. The length of Cu–$N_{amine}$ bond increase in the order: 2.222(2) Å **[$L_F$CuCl$_2$]** < 2.367(3) Å **[$L_A$CuCl$_2$]** < 2.368(3) Å **[$L_B$CuCl$_2$]** < 2.4458(1) Å **[$L_C$CuCl$_2$]**. Substituents at the *para* position of the aniline moiety exert electronic effects on the Cu–$N_{amine}$ bond lengths in **[$L_n$CuCl$_2$]** ($L_n$ = $L_A$–$L_C$ and $L_F$).

The $N_{pyrazole}$–Cu–$N_{pyrazole}$ angles are 155.32(1)° **[$L_A$CuCl$_2$]**, 155.94(5)° **[$L_B$CuCl$_2$]**, 154.77(5)° **[$L_C$CuCl$_2$]**, and 159.64(9)° **[$L_F$CuCl$_2$]**. These angles are slightly affected by the steric bulk of the aniline substituents. The $N_{pyrazole}$–Cu–$N_{pyrazole}$ angles increase according to the increasing *para* substituents in the order H < F < OMe < $CH(CH_3)_2$. The Cl–Cu–Cl, $N_{amine}$–Cu–$N_{pyrazole}$, and $N_{pyrazole}$–Cu–Cl angles lie in the ranges 124.43(3)–143.91(2)°, 77.59(5)–79.93(8)°, and 92.83(4)–96.85(7)°, respectively. These values do not substantially vary from the expected values. Furthermore, the angles between the aromatic substituent plane and the bis-pyrazole plane are 42.78° for **[$L_A$CuCl$_2$]**, 47.22° for **[$L_B$CuCl$_2$]**, 43.12° for **[$L_C$CuCl$_2$]**, and 35.5° for **[$L_F$CuCl$_2$]**.

By contrast, **[$L_D$CuCl$_2$]** exhibited four-coordination geometry involving two nitrogen atoms of pyrazole moieties and two chloro ligands, resulting in an eight-membered chelate ring (**Fig. 4**) [36]. In **[$L_D$CuCl$_2$]**, the Cu(II) center in ligated to *N*,*N*-bis((3,5-dimethyl-1H-pyrazol-1-yl)methyl)-2,4,6-trimethylaniline and adopted a distorted tetrahedral geometry. These results suggest that the presence of methyl substituents at the *ortho* position steers the coordination mode and resultant geometries of the synthesized Cu(II) complexes. The average Cu–$N_{pyrazole}$ and Cu–Cl bond lengths are 2.002(2) and 2.243(8) Å, respectively, whereas the $N_{amine}\cdots$Cu distance is 2.954 Å. The bond angles of $N_{pyrazole}$–Cu–$N_{pyrazole}$ and Cl–Cu–Cl are 145.27(8)° and 139.96(3)° in **[$L_D$CuCl$_2$]**, respectively.

The $\tau_5$ values provide useful information about the geometry of five-coordinate complexes, i.e., complexes with an ideal square pyramidal geometry are characterized by a value for $\boldsymbol{\tau_5}$ of zero, on the other hand the value of $\boldsymbol{\tau_5}$ is equal to one in the case of an ideal trigonal bipyramidal geometry [51]. A comparison of the $\boldsymbol{\tau_5}$ parameter of the Cu(II) complexes synthesized in the present study are listed in **Table 2**. Based on the $\tau_5$ values the geometry around the Cu(II) center in **[$L_n$CuCl$_2$]** ($L_n$ = $L_A$–$L_C$ and $L_F$), can be described as distorted square-pyramidal consisting of three nitrogen atoms of pyrazolyl-methylamine framework and two Cl atoms. The plane angles between N2–Cu1–

N5 and Cl1–N3–Cl2 and between N2–Cu1–N4 and Cl1–N3–Cl2 in **[$L_B$CuCl$_2$]** and **[$L_C$CuCl$_2$]** are distorted by approximately 89.50° and 89.60°, respectively.

The new geometric parameters for the four-coordinate compounds ($\tau_4$) as improved simple metrics for quantitatively evaluating the geometry are presented in **Table 3** [52]. The $\tau_4$ values for a perfect tetrahedron and perfect square-planar geometry are 1.00 and zero, respectively. The degrees of distortion based on bond angles around the Cu(II) centers of the complexes prepared in the present work were evaluated using these structural indexes. The $\tau_4$ value of **[$L_D$CuCl$_2$]** is 0.531, which is closer to 1 than to zero. Thus, the geometry of **[$L_D$CuCl$_2$]** is best described as a distorted tetrahedron geometry. The plane angle between the Cl2–Cu1–Cl1 and $N_{pyrazole}$–Cu1–$N_{pyrazole}$ planes in **[$L_D$CuCl$_2$]** is calculated as 51.37°. Thus, variation in the steric bulk at the *ortho* position of the aniline moiety strongly affects the resultant geometry of these Cu(II) complexes.

*3.3. MMA polymerization*

In our continuing effort to design effective and stereoselective bis(pyrazolyl amine)-based PMMA catalysts, we assessed the catalytic performance of the Cu(II) complexes supported by bis((3,5-dimethyl-1*H*-pyrazol-1-yl)methyl)amines in MMA polymerization. Representative polymerization results are listed in **Table 4**. Polymerization data indicate that all synthesized Cu(II) complexes polymerized MMA, yielding PMMA with a $T_g$ between 122 and 128 °C. The polymers were isolated as white powders and were characterized by GPC using polystyrene standards as a reference and THF as the eluent.

Notably, **[$L_F$CuCl$_2$]** exhibited the highest catalytic activity ($2.81 \times 10^4$ g (mol Cu)$^{-1}$ h$^{-1}$) and produced PMMA with molecular weight ($2.27 \times 10^5$ g mol$^{-1}$) compared to rest of its analogous. The steric bulk of the substituents at the *ortho* position of the aniline moiety influenced the catalytic performance of the Cu(II) complexes. For instance, when the ethyl (–$CH_2CH_3$) group attached at the

*ortho* position of the aniline moiety in **[$L_ECuCl_2$]** changed to $-CH_3$ (in **[$L_DCuCl_2$]**) and –H (in **[$L_CCuCl_2$]**) groups, an increase in MMA activity was observed (**Table 4**). A trivial tendency between the steric bulk and catalytic capabilities in complexes bearing alkyl groups attached at the *ortho* position of the aniline moiety was observed to be in the order of $-CH_2CH_3$ < $-CH_3$ < –H (**Table 4**). The presence of an ethyl group at the *ortho* position increases the steric demand of the ligand, thus decreasing the size of the possible reaction site. However, the electron-donating character of the alkyl moieties lowers the Lewis acidity of the metal center. The metal is thus less activating and thereby hinders the polymerization. As evident from our previous report, bulky substituents attached to amine or pyrazole moieties negatively affect MMA activation; in this case, the steric clashes between the attached ligands and the incoming monomer likely impede the monomer's approach to the metal site [53]. These results are in contrast to our previous results, which indicated that an increase in steric bulk at pyrazole and aniline moieties corresponded to greater polymerization activities [32]. However, despite of the lower steric bulk at *ortho* positions, **[$L_ACuCl_2$]** and **[$L_BCuCl_2$]** exhibited lower activities. These surprising results with respect to steric bulk and the observed activities are difficult to explain. It is evident from polymerization data that **[$L_FCuCl_2$]** exhibited the highest catalytic activity compared to rest of its analogous. The presence of fluoro substituent at *para* position of aniline moiety in **[$L_FCuCl_2$]** might impend the electron withdrawing effect enhancing Lewis acid strength of metal centre. Additionally, the presence of less sterically bulky substituent (-H) at *ortho* position and better solubility of **[$L_FCuCl_2$]** can also be attributed to its better performance in term of activity. The PDI values of PMMA obtained with the Cu(II) complexes ranged from 1.42 to 1.61 at 60 °C. The molecular weights of the resultant PMMAs were not significantly affected by steric bulk of the substituents of the aniline moieties. Furthermore, the mediocre activities of our current system can be ascribed to their low solubility in the polymerization media.

In comparison with our previously reported five-coordinated Cu(II) complexes bearing *N*,*N*-bis((3,5-dimethyl-1*H*-pyrazol-1-yl)methyl)cyclopentanamine [54] and *N*-methyl-*N*-((pyridine-2-yl)methyl)benzeneamine [56], the current catalytic system exhibits slightly higher activities and stereoselectivities, yielding PMMA with lower molecular weights. Similarly, compared with previously reported four-coordinated Zn(II) and Co(II) complexes with *N*,*N*′,*N*-bis((1*H*-pyrazol-1-yl)methyl)amine derivatives [54], **[$L_D$CuCl$_2$]** with a four-coordination structure exhibits lower activity and yields PMMA with identical stereoselectivity.

The blank polymerization of MMA was carried out using starting materials, i.e., $CuCl_2 \cdot 2H_2O$/MMAO or solely MMAO, under identical experimental conditions to evaluate the ligand effect on the central metal atom. The polymerization data clearly show that the $CuCl_2 \cdot 2H_2O$/MMAO system exhibited lower activities and stereoselectivities and yielded PMMA with comparable molecular weights. Similarly, in the case of MMAO, the activity and stereoselectivity were lower than **[$L_n$CuCl$_2$]**/MMAO systems. Attempts to induce polymerization with dichloro Cu(II) complexes in the absence of MMAO were unsuccessful.

Isotactic PMMA, which is produced through radical processes commercially, has a $T_g$ value of approximately 65 °C [56]. Recent advancements have been focused on preparing PMMA with a high $T_g$ and improved properties *via* non-radical MMA polymerization catalyzed by coordination complexes. The syndiotactic enchainment ranged from 0.66 to 0.68 in almost all cases, irrespective of the catalysts' coordination modes and activities. The syndiotacticity of the resultant PMMA was not strongly affected by variation of the aniline substituents. Importantly, the resultant syndiotactic enchainment was not sufficiently high to enable us to predict the mechanism of coordination polymerization for the catalytic species in the present work. Future work will be focused on ligand modification to improve the catalytic performance and the resultant stereocontrol of the MMA polymerization.

*3.4. rac-Lactide polymerization*

ROP in a controlled and selective manner is a useful approach towards the synthesis of biodegradable polymers [57]. In this regard the *in situ* generated dimethyl Cu(II) species were investigated for their catalytic efficacies in the ROP of *rac*-LA at 25 °C. All the dimethyl Cu(II) species effectively catalyzed *rac*-LA polymerization, and the complete conversion of *rac*-LA to PLA was confirmed by the absence of the monomer signal in the $^1$H NMR spectrum (**Figure S15**). Representative polymerization results are summarized in **Table 5**.

The experimental $M_n$ values (corrected using a Mark–Houwink factor of 0.58) [58,59] determined with GPC were in agreement with theoretical values, suggesting polymerization at a single reaction site provided by the dimethyl Cu(II) complexes. Polymerization data indicate that PLAs obtained with **[$L_n$CuMe$_2$]** ($L_n$ = $L_A$–$L_F$) have broader PDIs, which might be a consequence of backbiting or transesterification side reactions, resulting in the formation of macrocycles with a wide molecular-weight distributions (MWD). When dichloro Co(II) complexes, **[$L_n$CuCl$_2$]** ($L_n$ = $L_A$ – $L_F$), were utilized as catalysts under the same experimental conditions; *rac*-LA polymerization was not initiated. Inspecting the $^1$H NMR spectra of the an isolated PLAs we were able to infer that the polymers are end-capped, with an –C(=O)CH$_3$ group at one terminus overlapped with those of PLA backbones and a hydroxyl group –CHMe–(OH) at the other (**Figure S17**). The coordination insertion mechanism [60,61] can be invoked for the ROP of *rac*-LA by these initiators. With this mechanism, *rac*-LA initially coordinates to the M(II) centre, yielding a penta-coordinated intermediate, followed by cleavage of the acyl-oxygen bond to open the monomer ring. Another molecule of *rac*-LA gets opened by attaching to the M(II) centre in a similar manner. The successive addition of monomer produces a hetero-enriched PLA.

Variation of the substituents at the *ortho* position of the aniline moiety did not affect the activity of the Cu(II) complexes at room temperature. However, the preliminary polymerization data obtained at -25 °C using dimethyl Cu(II) species showed that $\mathbf{L_D}$ containing complex exhibited the highest activity (**Table S2**; entry 5). The order of activity with respect to *ortho* substituents follow the order; $\mathbf{[L_DCuCl_2]} > \mathbf{[L_ECuCl_2]} > \mathbf{[L_FCuCl_2]}$ at -25 °C (**Table S2; entries 5-7**). It is presumed that the electron-donating character of the methyl moieties increases the electronic density around the metal center. Therefore, the metal is more activated, thereby promoting the polymerization. More detailed investigation is underway that is aimed at improving the Cu(II) complexes' catalytic activity and stereoselectivity through modification of the ligand framework at low temperatures.

On the basis of comparisons with previously reported values, the PLA produced by $\mathbf{[L_nCuMe_2]}$ ($L_n$ = $L_A$–$L_F$) was concluded to be predominantly heterotactic. The polymerization temperature apparently influenced the alternative insertion of *rac*-LA and the resultant microstructures of the PLA. The probability of heterotactic enchainment ($P_r$ values) ranged from 0.72 to 0.78 at 25 °C. However, a decrease in temperature from 25 to −25 °C resulted in increased heterotacticity ($0.84 \leq P_r \leq 0.90$) (**Table S2**). These results are consistent with our previous findings. No regular trend in heterotacticity was observed, suggesting that substituents at the *para* and *ortho* positions of the aniline less significantly affected the heterotacticity in the ROP of *rac*-LA.

The activities of the current system toward *rac*-LA at 25 °C are higher that the activities of our previously reported dimethyl complexes with comparable heterotacticity [62,63]. *Nacnac*$^{Bn}$CuO$^{i}$Pr, a recently reported, highly active catalyst for the ROP of LA, produced PLA with almost no stereocontrol [64]. Compared with the highly effective Cu(II) initiators based on *N*-(pyridin-2-ylmethyl)amine [36], the current Cu(II) systems exhibit lower catalytic efficacy but produce PLA with better heterotacticity and PDIs.

## 4. Conclusions

In summary, we demonstrated the synthesis and X-ray crystallographic structures of **[$L_nCuCl_2$]** ($L_n$ = $L_A$–$L_F$) supported by bis((3,5-dimethyl-1*H*-pyrazol-1-yl)methylamine derived ligands. In **[$L_nCuCl_2$]** ($L_n$ = $L_A$–$L_C$ and $L_F$), the Cu(II) center is coordinated to pyrazole and amine nitrogen atoms along with two chloro ligands, displaying a five-coordinated distorted square-pyramidal geometry. However, the **[$L_DCuCl_2$]** with four-coordination mode adopted a distorted tetrahedron geometry. Investigation of the catalytic efficacy of synthesized Cu(II) complexes in MMA polymerization revealed **[$L_FCuCl_2$]** ($2.81 \times 10^4$ g PMMA/mol Cu h) to display promising catalytic activity and furnished syndio-enriched PMMA. The activities of the studied Cu(II) complexes varied with respect the substituents of the aniline moiety. Additionally, *in situ* generated dimethyl Cu(II) complexes demonstrated high activities toward *rac*-LA, and furnished PLAs with mediocre heterotacticity with slightly higher PDI values. Notably, the activities of the catalyst for MMA and *rac*-LA polymerization was observed to be influenced by the steric and electronic properties of the ligand attached to metal center.

## Supplementary Materials

CCDC 1903792 – 1903796 contains the supplementary crystallographic data for **[$L_ACuCl_2$]**, **[$L_BCuCl_2$]**, **[$L_CCuCl_2$]**, **[$L_DCuCl_2$]·$CH_2Cl_2$** and **[$L_FCuCl_2$]·$3CH_2Cl_2$,** respectively. These data can be obtained free of charge *via* http://www.ccdc.cam.ac.uk/conts/retrieving.html or from the Cambridge Crystallographic Data Centre, 12 Union Road, Cambridge CB2 1EZ, UK; fax: (+44) 1223-336-033; or e-mail: deposit@ccdc.cam.ac.uk.

## Conflicts of Interests

There are no conflicts to declare.

**Acknowledgments**

This research was supported by the National Research Foundation (NRF) of South Korea, funded by the Ministry of the Education, Science, and Technology (MEST) (Grant No. 2019R1A2C1088654). X-ray crystallography with PLS-II 2D-SMC beamline was supported by MSIP and POSTECH.

**References**

[1] Y.C.M. Pennings, W.L. Driessen, J. Reedijk, Polyhedron 7 (1988) 2583-2589.

[2] N. Ajellal, M.C.A. Kuhn, A.D.G. Boff, M. Hoerner, C.M. Thomas, J.-F. Carpentier, O.L., Jr. Casagrande, Organometallics 25 (2006) 1213-1216.

[3] S.S. Massoud, F.R. Louka, R.N. David, M.J. Dartez, Q.L. Nguyn, N.J. Labry, R.C. Fischer, F. A. Mautner, Polyhedron 90 (2015) 258-265.

[4] B. Lian, C.M. Thomas, O.L. Casagrande Jr., C.W. Lehmann, T. Roisnel, J.-F. Carpentier, Inorg. Chem. 46 (2007) 328-340.

[5] A. John, M.M. Shaikh, R.J. Butcher, P. Ghosh, Dalton Trans. 39 (2010) 7353-7363.

[6] D.L. Reger, E.A. Foley, M.D. Smith, Inorg. Chem. 48 (2009) 936-945.

[7] F. Xue, J. Zhao, T.S.A. Hor, Dalton Trans. 42 (2013) 5150-5158.

[8] P.K. Byers, A.J. Canty, R.T. Honeyman, Adv. Organomet. Chem. 34 (1992) 1-65.

[9] R. Mukherjee, Coord. Chem. Rev. 203 (2000) 151-218.

[10] W.L. Driessen, Recl. Trav. Chim. Pays-Bas 101 (1982) 441-443.

[11] F. Xue, J. Zhao, T.S.A. Hor, Dalton Trans. 40 (2011) 8935-8940.

[12] T.B. Hadda, A.T. Kotchevar, M. Daoudi, B. Bennani, N.B. Larbi, A. Kerbal, Lett. Drug Des. Discov. 2 (2005) 584-589.

[13] I. Bouabdallah, L.A. M'barek, A. Zyad, A. Ramdani, I. Zidane, A. Melhaoui, Nat. Prod. Res. 20 (2006) 1024-1030.

[14] J. Hitzbleck, A.Y. O'Brien, G.B. Deacon, K. Ruhlandt-Senge, Inorg. Chem. 45 (2006) 10329-10337.

[15] J. Gätjens, C.S. Mullins, J.W. Kampf, P. Thuéryb, V.L. Pecoraro, Dalton Trans. (2009) 51-62.

[16] T. Hanif, F. Malek, B.E. Ball, A. Khan, K. Dalvandi, B.P. Marasini, S. Noreen, R. Malik, S. Khan, M.I. Choudhary, Med. Chem. Res. 21 (2012) 2772-2778.
[17] Z. Jian, W. Zhao, X. Liu, X. Chen, T. Tang, D. Cui, Dalton Trans. 39 (2010) 6871-6876.
[18] V.C. Gibson, C.M. Halliwell, N.J. Long, P. J. Oxford, A.M. Smith, A.J.P. White, D.J. Williams, Dalton Trans. (2003) 918-926.
[19] A. Sood, M.T. Räisänen, E. Aitola, A. Sibaouih, E. Colacio, M. Ahlgren, M. Nieger, T. Repo, M. Leskelä, Polyhedron 56 (2013) 221-229.
[20] L.L. de Oliveira, R.R. Campedelli, M.C.A. Kuhn, J.-F. Carpentier, O.L. Casagrande Jr, J. Mol. Catal. A-Chem. 288 (2008) 58-62.
[21] X. Guan, X. Ma, H. Zhou, F. Chen, Z. Li, J. Thermoplast. Compos. Mater. 30 (2017) 691-706.
[22] L.-L. Miao, H.-X. Li, M. Yu, W. Zhao, W.-J. Gong, J. Gao, Z.-G. Ren, H.-F. Wang, J.P. Lang, Dalton Trans. 41 (2012) 3424-3430.
[23] H.-Y. Ding, H.-J. Cheng, F. Wang, D.-X. Liu, H.-X. Li, Y.-Y. Fang, W. Zhao, J.-P. Lang, J. Organomet. Chem. 741 (2013) 1-6.
[24] D.H. Camacho, Z. Guan, Chem. Commun. 46 (2010) 7879-7893.
[25] S.D. Ittel, L.K. Johnson, M. Brookhart, Chem. Rev. 100 (2000) 1169-1204.
[26] S. Meking, Angew. Chem., Int. Ed. 40 (2001) 534-540.
[27] S. Fortun, P. Daneshmand, F. Schaper, Angew. Chem. Int. Ed. 54 (2015) 13669-13672.
[28] P. Daneshmand, A. van der Est, F.Schaper, ACS Catal. 7 (2017) 6289-6301.
[29] S. Shin, H. Cho, H. Lee, S. Nayab, Y. Kim, J. Coord. Chem. 71 (2018) 556-584.
[30] M. Yang, W.J. Park, K.B. Yoon, J.H. Jeong, H. Lee, Inorg. Chem. Commun. 14 (2011) 189-193.
[31] D. Kim, S. Kim, H.Y. Woo, H.-J. Lee, H. Lee, Appl. Organomet. Chem. 28 (2014) 445 -453.
[32] S. Choi, S.H. Ahn, S. Nayab, H. Lee, Inorg. Chimi. Acta 435 (2015) 313-319.
[33] S. Choi, S. Nayab, J. Jeon, S.H. Park, H. Lee, Inorg. Chimi. Acta 438 (2015)118-127
[34] S.H. Ahn, M.K. Chun, E. Kim, J.H. Jeong, S. Nayab, H. Lee, Polyhedron 127 (2017) 51-58.
[35] X.F. Yu, C. Zhang, Z.X. Wang, Organometallics 32 (2013) 3262-3268.
[36] Y.K. Kang, J.J. Jeong, N.Y. Lee, Y.T. Lee, H. Lee, Polyhedron 29 (2010) 2404-2408.
[37] I. Dvoretzky, G.H. Richter, J. Org. Chem. 15 (1950) 1285-1288.
[38] S. Shin, S. Nayab, H. Lee, Polyhedron 141 (2018) 309-321.
[39] S. Shin, S.H. Ahn, M.J. Jung, S. Nayab, H. Lee, J. Coord. Chem. 69 (2016) 2391-2402.
[40] A. S. Brar, G. Singh, R. Shanker. J. Mol. Struct. 703 (2004) 69-81.
[41] T. Konishi, Y. Tamai, M. Furn, Y. Einaga, H. Yamakawa, Polym. J. 21 (1989) 329-340.

[42] F. Drouin, T.J.J. Whitehorne, F. Schaper, Dalton Trans. 40 (2011) 1396-1400.

[43] M.T. Zell, B.E. Padden, A.J. Paterick, K.A.M. Thakur, R.T. Kean, M.A. Hillmyer, E.J. Munson, Macromolecules 35 (2002) 7700-7707.

[44] J.W. Shin, K. Eom, D. Moon, BL2D-SMC, J. Synchrotron Rad. 23 (2016) 369-373.

[45] Z. Otwinowski, W. Minor, in: C.W Carter Jr., R.M. Sweet (Eds.), Methods in Enzymology Academic Press, New York 276 (1997) 307-326.

[46] SMART and SAINT-Plus v 6.22, Bruker AXS Inc., Madison, Wisconsin, USA (2000).

[47] G.M. Sheldrick, SADABS v 2.03, University of Göttingen, Germany (2002).

[48] G.M. Sheldrick, Acta Cryst. A71 (2015) 3-8.

[49] G.M. Sheldrick, Acta Cryst. C71 (2015) 3-8.

[50] M.H. Sadhu, S.B. Kumar, Synthesis, J. Mol. Struct. 1164 (2018) 239-247

[51] A.W. Addison, T.N. Rao, J. Reedijk, J. van Rijn, G.C. Verschoor, J. Chem. Soc., Dalton Trans. (1984) 1349-1356.

[52] L. Yang, D.R. Powell, R.P. Houser, Dalton Trans 9 (2007) 955-964.

[53] H. Cho, M.J. Jung, J. Jeon, H. Lee, S. Nayab, Inorg. Chimi. Acta 487 (2019) 221-227.

[54] Z. Zhang, W. Zhang, X. Zhu, Z. Cheng, J. Zhu, J. Polym. Sci. Part A (2007) 5722-5730.

[55] S.H. Ahn, H. Lee, Bull. Korean Chem. Soc. 37 (2016) 27-32

[56] I. A. Opeida, M. A. Kompanets, O. V. Kushch, E. S. Papayanina, Theor. Exp. Chem. 47 (2011) 30-35.

[57] J.-F. Lutz, M. Ouchi, D.R. Liu, M. Sawamoto, Science 341 (2013) 1238149.

[58] J.C. Wu, B.H. Huang, M.L. Hsueh, S.L. Lai, C.C. Lin, Polymer 46 (2005) 9784-9792.

[59] M.A. Masuelli, J. Polym. & Biopolym. Phys. Chem. 2 (2014) 37-43.

[60] H.R. Kricheldorf, S.R. Lee, S. Bush, Macromolecules 29 (1996) 1375-1381.

[61] N. Ajellal, D.M. Lyubov, M.A. Sinenkov, G.K. Fukin, A.V. Cherkasov, C.M. Thomas, J.F. Carpentier, A.A. Trifonov, Chem. Eur. J. 14 (2008) 5440-5448.

[62] S. Nayab, H. Lee, J.H. Jeong, Polyhedron 43 (2012) 55-62.

[63] S. Nayab, J.H. Jeong, Polyhedron 59 (2013) 138-143.

[64] T.J.J. Whitehorne, F. Schaper, Chem. Commun. 48 (2012) 10334-10336.

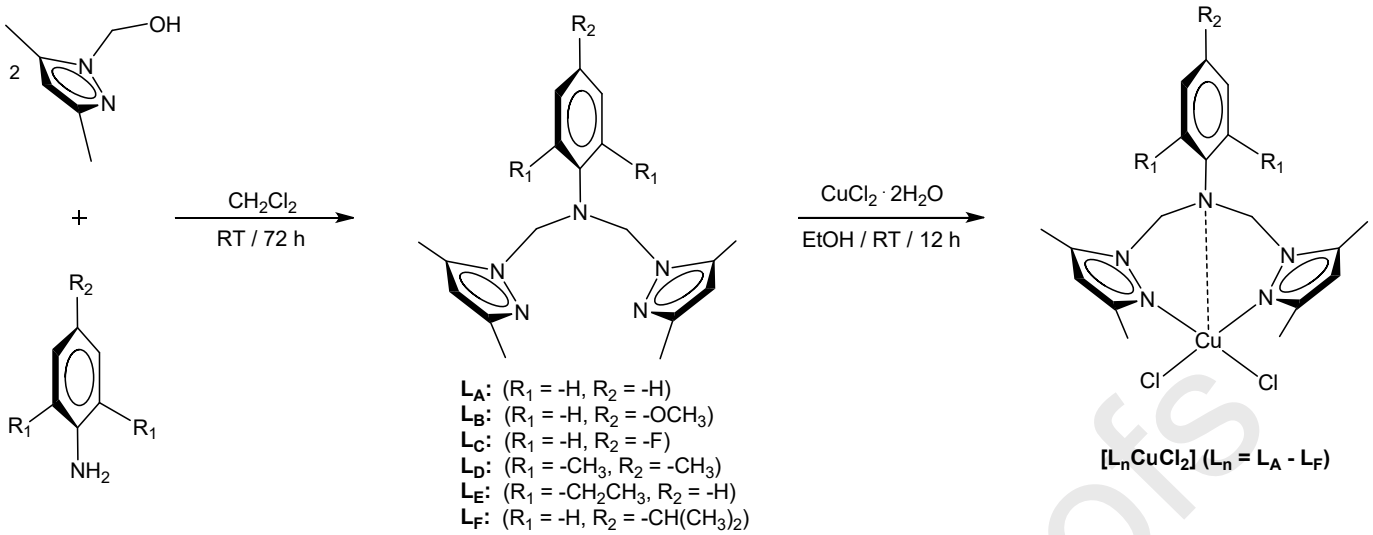


**Scheme 1.** Schematic representation of the synthesis of ligands ($L_n$ = $L_A$–$L_F$) and their corresponding Cu(II) complexes, **[$L_n$CuCl$_2$]** ($L_n$ = $L_A$–$L_F$).

**Table 1.** The selected bond lengths (Å) and angles (°) of **[$L_nCuCl_2$]** ($L_n$ = $L_A$–$L_D$ and $L_F$).

| **[$L_ACuCl_2$]** | | **[$L_BCuCl_2$]** | | **[$L_CCuCl_2$]** | | **[$L_DCuCl_2$]·$CH_2Cl_2$** | | **[$L_FCuCl_2$]·3$CH_2Cl_2$** | |
|---|---|---|---|---|---|---|---|---|---|
| **Bond lengths** (Å) | | | | | | | | | |
| Cu(1)-N(5) | 1.981(4) | Cu(1)-N(5) | 1.9898(2) | Cu(1)-N(4) | 1.9927(1) | Cu(1)-N(2) | 2.001(2) | Cu(1)-N(5) | 1.996(2) |
| Cu(1)-N(1) | 2.011(3) | Cu(1)-N(2) | 1.9965(2) | Cu(1)-N(2) | 2.0077(1) | Cu(1)-N(4) | 2.003(2) | Cu(1)-N(1) | 2.006(2) |
| Cu(1)-Cl(1) | 2.2703(1) | Cu(1)-Cl(1) | 2.2742(6) | Cu(1)-Cl(2) | 2.2652(5) | Cu(1)-Cl(1) | 2.2405(8) | Cu(1)-N(3) | 2.222(2) |
| Cu(1)-Cl(2) | 2.3052(1) | Cu(1)-Cl(2) | 2.2931(5) | Cu(1)-Cl(1) | 2.2902(6) | Cu(1)-Cl(2) | 2.2453(9) | Cu(1)-Cl(1) | 2.2568(9) |
| Cu(1)-N(5) | 1.981(4) | Cu(1)-N(5) | 1.9898(2) | N(1)-C(6) | 1.4543(2) | N(3)-C(7) | 1.444(3) | N(3)-C(1) | 1.464(3) |
| Cu(1)-N(3) | 2.367(3) | Cu(1)-N(3) | 2.3680(1) | Cu(1)-N(3) | 2.4458(1) | N(1)-C(3) | 1.350(3) | Cu(1)-Cl(2) | 2.3827(8) |
| N(1)-N(2) | 1.371(4) | N(1)-N(2) | 1.3657(2) | N(1)-C(3) | 1.3546(2) | N(1)-N(2) | 1.372(2) | N(1)-N(2) | 1.372(3) |
| **Bond angles** (°) | | | | | | | | | |
| N(5)-Cu(1)-N(1) | 155.32(1) | N(5)-Cu(1)-N(2) | 155.94(5) | N(4)-Cu(1)-N(2) | 154.77(5) | N(2)-Cu(1)-N(4) | 145.27(8) | N(5)-Cu(1)-N(1) | 159.64(9) |
| N(5)-Cu(1)-Cl(1) | 95.64(1) | N(5)-Cu(1)-Cl(1) | 95.97(4) | N(4)-Cu(1)-Cl(2) | 95.66(4) | N(2)-Cu(1)-Cl(1) | 96.53(6) | N(5)-Cu(1)-N(3) | 79.73(8) |
| N(1)-Cu(1)-Cl(1) | 96.85(1) | N(2)-Cu(1)-Cl(1) | 94.91(4) | N(2)-Cu(1)-Cl(2) | 94.83(4) | N(4)-Cu(1)-Cl(1) | 96.35(6) | N(1)-Cu(1)-N(3) | 79.93(8) |
| N(5)-Cu(1)-Cl(2) | 91.10(1) | N(5)-Cu(1)-Cl(2) | 92.89(4) | N(4)-Cu(1)-Cl(1) | 92.10(5) | N(2)-Cu(1)-Cl(2) | 94.97(6) | N(5)-Cu(1)-Cl(1) | 97.65(7) |
| N(1)-Cu(1)-Cl(2) | 95.24(1) | N(2)-Cu(1)-Cl(2) | 93.38(4) | N(2)-Cu(1)-Cl(1) | 92.83(5) | N(4)-Cu(1)-Cl(2) | 95.59(6) | N(1)-Cu(1)-Cl(1) | 96.58(7) |
| Cl(1)-Cu(1)-Cl(2) | 134.32(4) | Cl(1)-Cu(1)-Cl(2) | 133.72(2) | Cl(2)-Cu(1)-Cl(1) | 143.905(2) | Cl(1)-Cu(1)-Cl(2) | 139.96(3) | N(3)-Cu(1)-Cl(1) | 136.81(6) |
| N(5)-Cu(1)-N(3) | 77.83(1) | N(5)-Cu(1)-N(3) | 77.99(5) | N(4)-Cu(1)-N(3) | 77.84(5) | C(3)-N(1)-N(2) | 111.05(2) | N(5)-Cu(1)-Cl(2) | 91.83(7) |
| N(1)-Cu(1)-N(3) | 77.59(1) | N(2)-Cu(1)-N(3) | 78.03(5) | N(2)-Cu(1)-N(3) | 76.98(5) | C(3)-N(1)-C(6) | 127.80(2) | N(1)-Cu(1)-Cl(2) | 92.06(7) |

| | | | | | | | | | |
|---|---|---|---|---|---|---|---|---|---|
| Cl(2)-Cu(1)-N(3) | 99.99(8) | Cl(1)-Cu(1)-N(3) | 121.94(3) | Cl(2)-Cu(1)-N(3) | 118.17(4) | N(2)-N(1)-C(6) | 119.77(2) | N(3)-Cu(1)-Cl(2) | 98.77(6) |
| C(2)-N(1)-N(2) | 105.4(3) | Cl(2)-Cu(1)-N(3) | 100.34(4) | Cl(1)-Cu(1)-N(3) | 97.92(3) | C(1)-N(2)-N(1) | 106.01(2) | Cl(1)-Cu(1)-Cl(2) | 124.43(3) |
| C(2)-N(1)-Cu(1) | 140.0 (3) | C(3)-N(1)-N(2) | 111.65(1) | C(3)-N(1)-N(2) | 111.50(1) | C(1)-N(2)-Cu(1) | 134.38(2) | C(2)-N(1)-N(2) | 106.0(2) |

**Table 2.** Five-coordinate geometry indices ($\tau_5$) for **[$L_nCuCl_2$]** ($L_n$ = $L_A$–$L_C$ and $L_F$) and representative examples from the literature.

| Complexes | Geometry | $\tau_5$ | Reference |
|---|---|---|---|
| Trigonal bipyramidal ($D_{3h}$) | Trigonal bipyramidal | 1.000 | [51] |
| **[[$L_ACuCl_2$]** | Square pyramidal | 0.350 | This work |
| **[$L_BCuCl_2$]** | Square pyramidal | 0.370 | This work |
| **[$L_CCuCl_2$]** | Square pyramidal | 0.180 | This work |
| **[$L_FCuCl_2$]** | Square pyramidal | 0.381 | This work |
| Square pyramidal ($C_{4v}$) [a] | Square pyramidal | 0.000 | [51] |

See reference [51]

**Table 3.** Four-coordinate geometry indices ($\tau_4$) for **[$L_D$CuCl$_2$]** and representative examples from the literature.

| **Complexes** | **Geometry** | $\tau_4$ | **Reference** |
|---|---|---|---|
| Square planar ($D_{4h}$)[a] | Square planar | 0.00 | [52] |
| **[$L_D$CuCl$_2$]** | Tetrahedral | 0.531 | This work |
| Tetrahedral ($T_d$) [a] | Tetrahedral | 1.00 | [52] |

See reference [52]

**Table 4.** Polymerization of MMA by **[$L_nCuCl_2$]** ($L_n$ = $L_A$–$L_{F)}$ complexes in the presence of MMAO.

| Entry | Catalyst[a] | Yield[b] | Activity[c] | $T_g$[d] | Tacticity[e] | | | $M_w$[f] | $M_w/M_n$[f] |
|---|---|---|---|---|---|---|---|---|---|
| | | (g) | (g (mol-Cat)$^{-1}$ h$^{-1}$) × $10^4$ | (°C) | %*mm* | %*mr* | %*rr* | (g mol$^{-1}$) ×$10^5$ | |
| **1** | **$CuCl_2{\cdot}2H_2O$**[g] | 10.8 | 1.73 | 129 | 7.20 | 23.9 | 67.5 | 2.73 | 1.49 |
| **2** | MMAO[h] | 6.83 | 1.07 | 120 | 37.2 | 10.9 | 51.9 | 1.75 | 1.37 |
| **3** | **[$L_ACuCl_2$]** | 13.6 | 2.13 | 127 | 7.53 | 24.0 | 68.4 | 3.08 | 1.61 |
| **4** | **[$L_BCuCl_2$]** | 14.7 | 2.30 | 128 | 7.76 | 24.6 | 66.5 | 2.35 | 1.57 |
| **5** | **[$L_CCuCl_2$]** | 16.0 | 2.53 | 128 | 7.53 | 24.9 | 68.9 | 2.48 | 1.55 |
| **6** | **[$L_DCuCl_2$]** | 16.2 | 2.50 | 125 | 6.51 | 24.8 | 68.7 | 2.20 | 1.51 |
| **7** | **[$L_ECuCl_2$]** | 15.9 | 2.48 | 123 | 7.36 | 25.3 | 68.5 | 1.78 | 1.42 |
| **8** | **[$L_FCuCl_2$]** | 18.0 | 2.81 | 122 | 7.55 | 23.9 | 68.6 | 2.27 | 1.48 |

[a] $[Cu(II)\ catalyst]_0$ = 15 μmol, and $[MMA]_0/[MMAO]_0/[Cu(II)\ catalyst]_0$ = 3100:500:1, polymerization temp. = 60 °C, time = 2 h.

[b] Yield defined a mass of dried polymer recovered/mass of monomer used.

[c] Activity is calculated (g of PMMA)/(mol Cu·h).

[d] $T_g$ is the glass-transition temperature, which was determined using a thermal analyzer.

[e] The microstructural analysis of PMMA as syndiotactic (*rr*, 0.85 ppm), heterotactic (*mr*, 1.02 ppm), or isotactic (*mm*, 1.21 ppm) was carried out by $^1$H NMR [40,41].

[f] Determined by gel-permeation chromatography (GPC) eluted with THF at room temperature by filtration, with polystyrene calibration; $M_n$ refers the number average molecular weights of PMMA.

[g] Blank polymerization using $CuCl_2{\cdot}2H_2O$, also activated by MMAO.

[h] Blank polymerization carried out solely with MMAO.

**Table 5**. Polymerization of *rac*-LA with *in-situ*-generated dimethyl complexes at 25 °C.

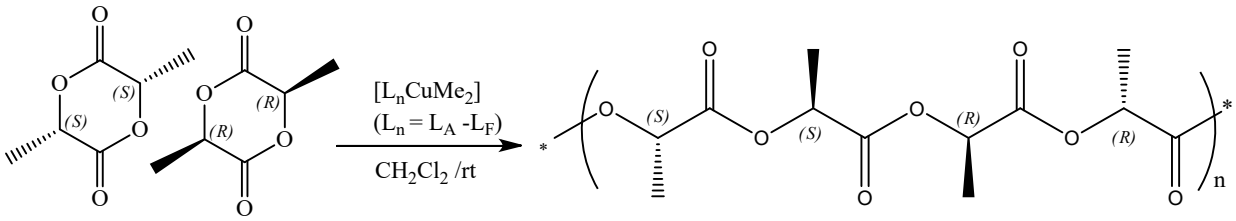


*rac*-lactide Heterotatic PLA

| Entry | Catalyst[a] | Conv.[b] (%) | $M_n$[c] (g mol$^{-1}$) × $10^3$ (calcd.) | $M_n$[d] (g mol$^{-1}$) × $10^3$ (GPC) | PDI[e] | $P_r$[f] |
|---|---|---|---|---|---|---|
| **1** | **MeLi** | 100 | 14.41 | 14.21 | 1.40 | 0.67 |
| **2** | **[$L_A$CuMe$_2$]** | 100 | 14.41 | 13.88 | 1.64 | 0.72 |
| **3** | **[$L_B$CuMe$_2$]** | 100 | 14.41 | 19.13 | 1.45 | 0.74 |
| **4** | **[$L_C$CuMe$_2$]** | 100 | 14.41 | 14.22 | 1.59 | 0.74 |
| **5** | **[$L_D$CuMe$_2$]** | 100 | 14.41 | 13.31 | 1.45 | 0.72 |
| **6** | **[$L_E$CuMe$_2$]** | 100 | 14.41 | 12.54 | 1.52 | 0.72 |
| **7** | **[$L_F$CuMe$_2$]** | 100 | 14.41 | 19.92 | 1.49 | 0.78 |

[a] Conditions: [Initiator] = 0.0625 mmol, [*rac*-LA]/[Cu-Initiator] = 100:1, 5.0 mL of $CH_2Cl_2$, time = 2 h, temp = 25 °C.

[b] Monomer conversion (%) determined by $^1$H NMR spectroscopy.

[c] Calculated from ([molecular weight of *rac*-LA] × [mol concentration of used *rac*-LA]/[mol concentration of copper initiator]) × (conversion).

[d] Experimental values (corrected using a Mark–Houwink factor of 0.58) [58,59].

[e] Determined by gel-permeation chromatography (GPC) in THF, relative to polystyrene standards.

[f] Probability of heterotactic enchainment ($P_r$) were calculated on the basis of homonuclear decoupled $^1$H NMR spectra according to a method reported elsewhere [42,43].

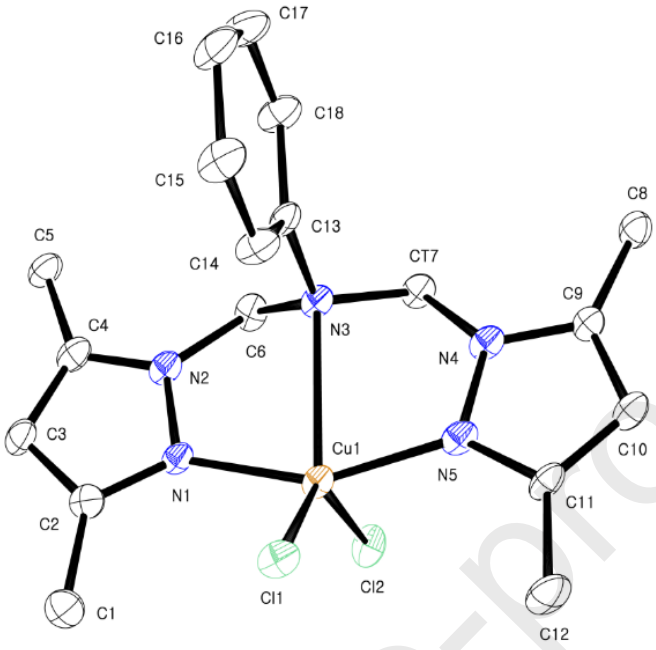


**Fig.1.** An ORTEP drawing of **[$L_A$CuCl$_2$]** with thermal ellipsoids at 50% probability. All hydrogen atoms have been omitted for clarity.

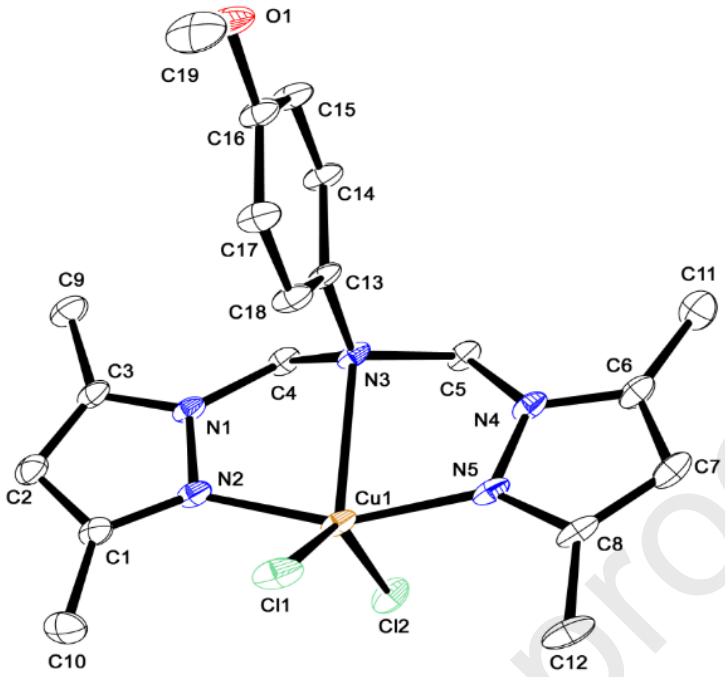


**Fig. 2.** An ORTEP drawing of **[$L_B$CuCl$_2$]** with thermal ellipsoids at 50% probability. All hydrogen atoms have been omitted for clarity.

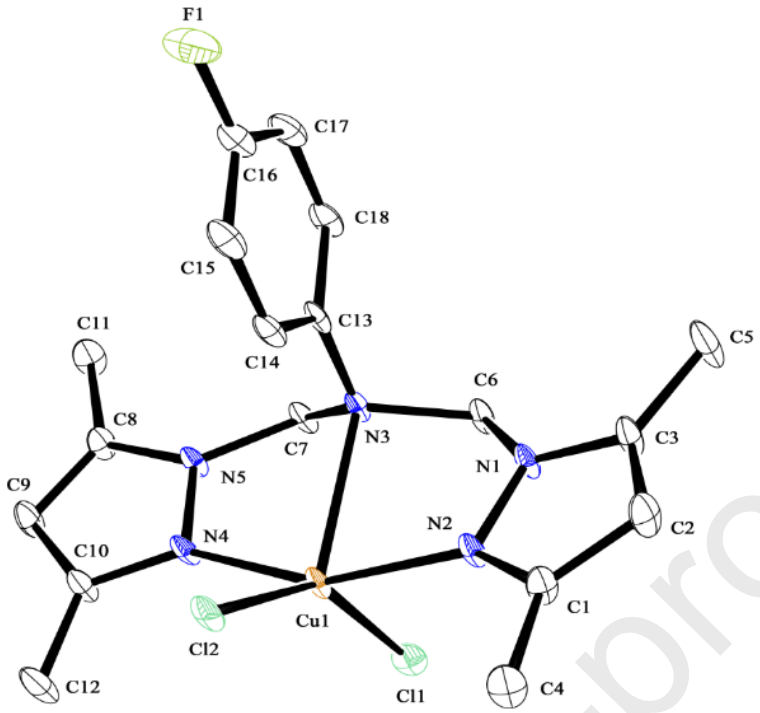


**Fig. 3.** An ORTEP drawing of **[$L_C$CuCl$_2$]** with thermal ellipsoids at 50% probability. All hydrogen atoms have been omitted for clarity.

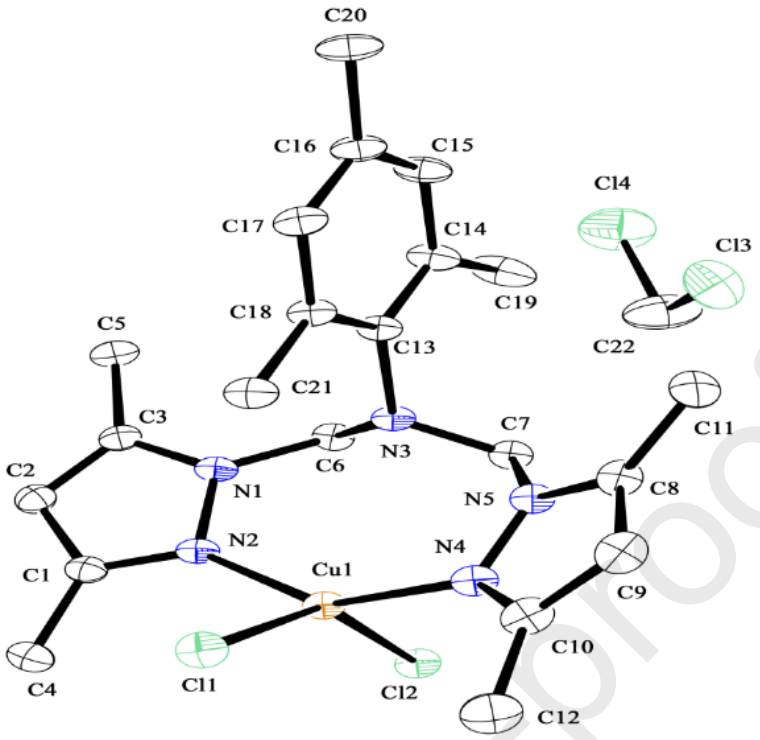


**Fig. 4.** An ORTEP drawing of **[$L_D$CuCl$_2$]**·**CH$_2$Cl$_2$** with thermal ellipsoids at 50% probability. All hydrogen atoms have been omitted for clarity.

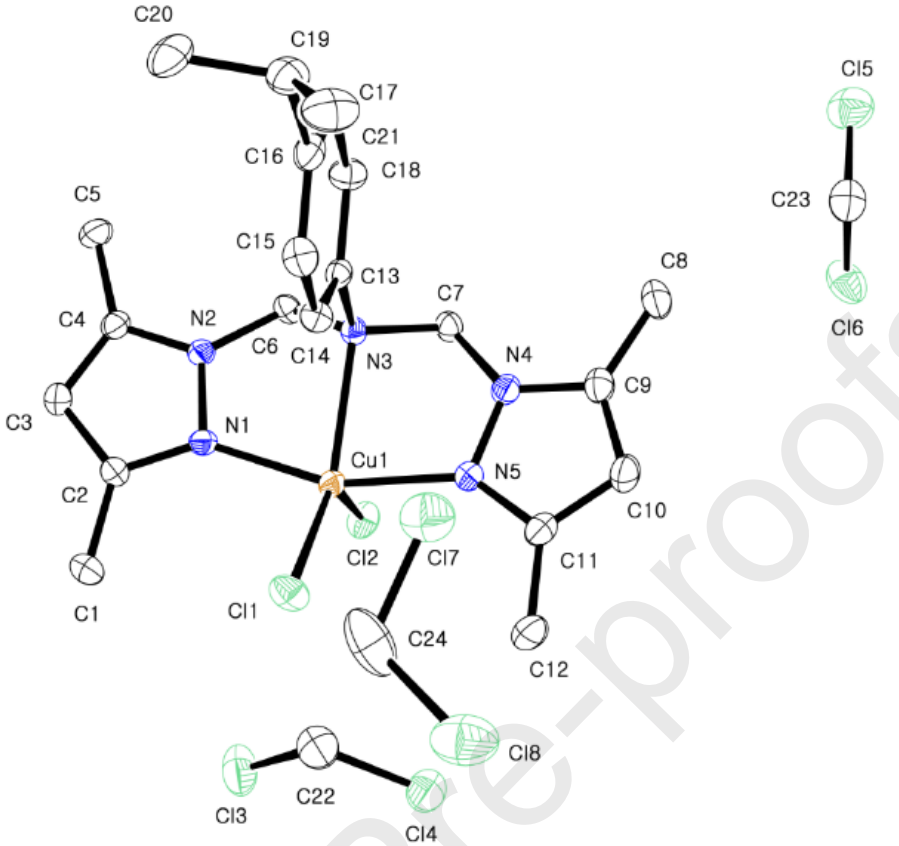


**Fig. 5.** An ORTEP drawing of **[$L_F$CuCl$_2$] · 3CH$_2$Cl$_2$** with thermal ellipsoids at 50% probability. All hydrogen atoms have been omitted for clarity.



# CRediT author statement

**Copper(II) Complexes Containing *N′*-Aromatic Group Substituted *N*,*N′*,*N*-bis((3,5-dimethyl-1H-pyrazol-1-yl)methyl)amines: Synthesis, Structures,**

# Polymerization of Methyl Methacrylate and Ring Opening Polymerization of *rac*-Lactide

**Hyungwoo Cho,[a] Solhye Choe,[a] Dongil Kim,[a] Hyosun Lee,[a,*] and Saira Nayab[b,*]**

**Hyungwoo Cho and Solhye Choe**: Visualization, Investigation. Experiments, Data collection.

**Dongil Kim**: Software, Validation.

**Hyosun Lee:** Conceptualization, Methodology, Software, Supervision, Writing- Reviewing and Editing.

**Saira Nayab.**: Data curation, Writing- Original draft preparation

**Declaration of interests**

☒ The authors declare that they have no known competing financial interests or personal relationships that could have appeared to influence the work reported in this paper.

☒ The authors declare the following financial interests/personal relationships which may

be considered as potential competing interests:

HYOSUN LEE



## Research Highlights

- Synthesis of bis((3,5-dimethyl-1*H*-pyrazol-1-yl)methyl)amines based Cu(II) complexes
- *N*′,*N*′- and *N*,*N*′,*N*′- coordination modes have been exhibited by these Cu(II) complexes
- Stereoselective ROP of *rac*-LA generates PLA with mediocre heterotacticity at 25 °C
- These complexes proved to be effective in the polymerization of MMA at 60 °C
- Syndio-enriched PMMAs with high molecular weights have been furnished

**Graphical Abstract**

The employment of bis((3,5-dimethyl-1H-pyrazol-1-yl)methyl)amines derivatives with $CuCl_2.2H_2O$, furnished Cu(II) complexes, **$[L_nCuCl_2]$** ($L_n = L_A - L_F$). X-ray diffraction studies revealed that variation of substituents at aniline moiety resulted in *N*,*N*′-bi and/or *N*,*N*′,*N*″-tridentate coordination modes with diverse geometries around the Cu(II) center. These complexes demonstrated moderate to high activities in MMA polymerization and furnished syndiotactic PMMA. Hetero-enriched PLAs have also been furnished by dimethyl derivatives of these Cu(II) complexes.

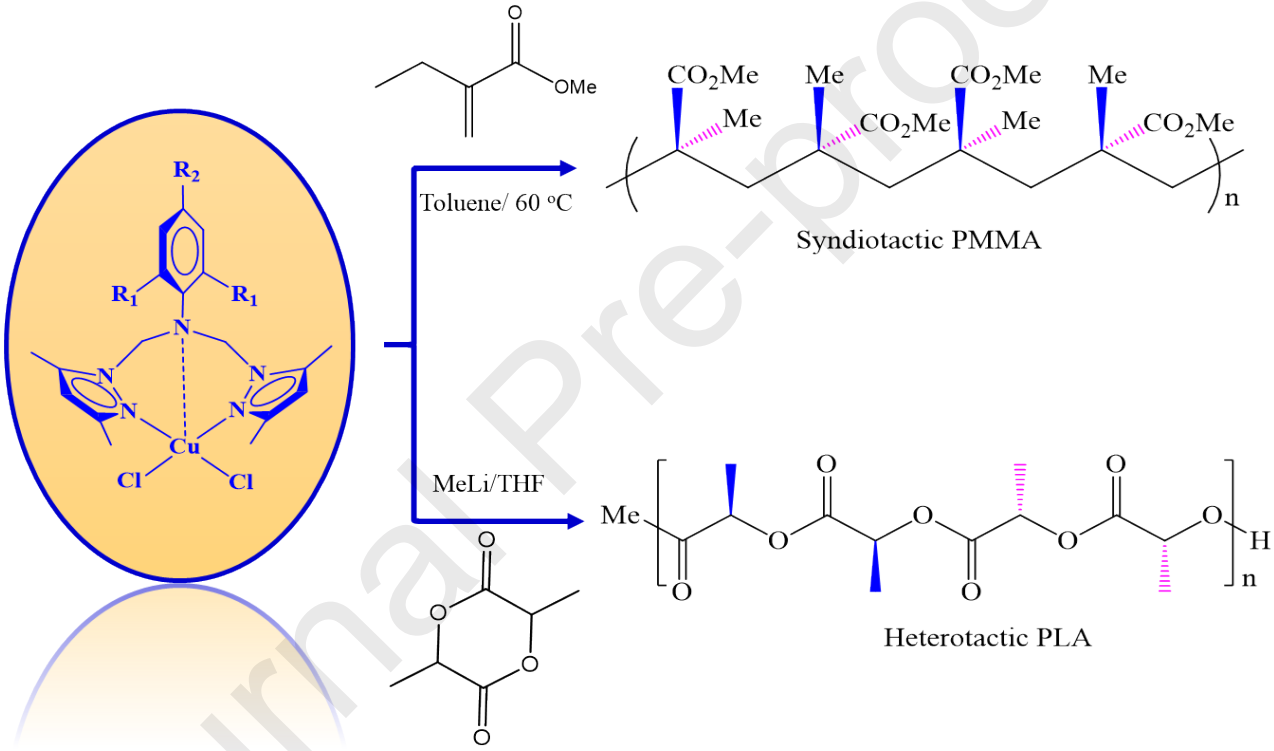


## Graphical Abstract

The employment of bis((3,5-dimethyl-1H-pyrazol-1-yl)methyl)amines derivatives with $CuCl_2.2H_2O$, furnished Cu(II) complexes, **$[L_nCuCl_2]$** ($L_n = L_A - L_F$). X-ray diffraction studies revealed that variation of substituents at aniline moiety resulted in *N*,*N*′-bi and/or *N*,*N*′,*N*″-

tridentate coordination modes with diverse geometries around the Cu(II) center. These complexes demonstrated moderate to high activities in MMA polymerization and furnished syndiotactic PMMA. Hetero-enriched PLAs have also been furnished by dimethyl derivatives of these Cu(II) complexes.